Theoretical investigation of the C_{60} infrared spectrum

Jaroslav Fabian
Department of Physics, State University of New York at Stony Brook, Stony Brook, New York 11794-3800
(Received 3 October 1995)

A semiempirical model of the infrared (IR) spectrum of the C_{60} molecule is proposed. The weak IR-active modes seen experimentally in a C_{60} crystalline sample are argued to be combination modes caused by anharmonicity. The origin of these two-mode excitations can be either mechanical (anharmonic interatomic forces) or electrical (nonlinear dipole-moment expansion in normal mode coordinates). It is shown that the electrical anharmonicity model exhibits basic features of the experimental spectrum while nonlinear dynamics would lead to a qualitatively different overall picture. [S0163-1829(96)08119-2]

I. INTRODUCTION

There has been a great deal of progress in our understanding of the chemistry and physical properties of fullerenes. The discovery of superconductivity in alkali-metal–doped C_{60} (Ref. 1) has ignited discussions on possible mechanisms of this phenomenon.[2,3] One class of models stresses the coupling between electrons and intramolecular phonons.[2] Raman and infrared (IR) spectroscopy have probed the vibrational properties of C_{60} compounds[4–10] and many theoretical models have tried to explain properties of the 46 distinct modes predicted by group theory.

The icosahedral (I_h) symmetry of C_{60} allows four distinct IR-active modes (T_{1u}) and ten Raman-active modes ($2A_g \oplus 8H_g$) in harmonic approximation. It is customary to denote the IR modes at frequencies 528, 577, 1183, and 1429 cm^{-1}, as $T_{1u}(i)$, $i=1,2,3,4$, respectively. 32 optically inactive (silent) modes are $1A_u$, $3T_{1g}$, $4T_{2g}$, $5T_{2u}$, $6G_g$, $6G_u$, and $7H_u$. Higher-order peaks are seen experimentally by increasing the optical depth of a sample. In principle there are 380 second-order combination modes IR allowed by the I_h symmetry.[8] Second-order overtones are IR forbidden.

Several authors reported observation of weak modes in Raman[10,11] and IR (Refs. 7–9 and 12) spectroscopy. Wang *et al.*,[7] Martin *et al.*,[8] and Kamarás *et al.*[9] analyzed the weakly active features in conjunction with Raman[10] and neutron measurements[13] to extract the 32 fundamental frequencies of the silent modes. The frequencies differ significantly among the authors, leaving the question of the assignment of fundamentals open.

Possible mechanisms of activating the weak modes include ^{13}C isotopic impurities, crystal environment effects, and anharmonicity. Impurities, dislocations, and electric field gradients at surface boundaries can be excluded due to their sample dependence. An experimental and theoretical vibrational study of ^{13}C-enriched crystals excluded the isotopic symmetry breaking as a potential candidate.[14] A few of the weak modes are thought to be activated due to the fcc crystal field effect. The crystal field reduces the I_h symmetry of C_{60} and activates silent odd-parity modes. Above 260 K the C_{60} molecules freely rotate and the time-averaged crystal field perturbation is zero. This effect of ''motional diminishing'' of silent modes has been experimentally observed and theoretically studied by Mihaly and Martin.[15] An experimental study of pressure dependence of these modes would help to substantiate this mechanism.

The goal of the present paper is to identify, qualitatively, the mechanism of activation of the higher-order vibrations; detailed assignment to normal modes remains a task for the future. The basic formalism of anharmonic effects on IR activity is given in Refs. 16–21. There are two ways in which anharmonicity can display itself in an optical spectrum. It is driven either by anharmonic interatomic forces (mechanical anharmonicity) or by an anharmonic coupling of a photon field to two or more phonons (electrical anharmonicity). Although the two mechanisms are not independent, each has its own characteristic absorption intensity pattern. When compared with an experimental spectrum one can decide which of the two kinds of anharmonicity prevails in the IR spectrum of C_{60}. Although the spectrum may contain cross contributions from both phenomena, here they are treated separately.

Several models have been used to calculate absorption intensities in harmonic approximation. Tight-binding models[22,23] are in complete disagreement with the experimental results. The bond-charge model[24] fits very well with frequency positions of fundamentals but the IR intensity pattern disagrees with basic trends in the observed spectrum. The same is true for a Hubbard-type model stressing electronic correlation effects.[25] Relative intensities are best reproduced by the local density approximation (LDA).[23,26] Due to its computational complexity the LDA scheme is not convenient for computing second-order intensities. We therefore propose a semiempirical model that is satisfactory for a qualitative comparison with experiment. Figure 1 summarizes the performance of these models in calculating the absorption intensities.

Some characteristics of the experimental IR spectrum[8] are shown in Fig. 2. Combination (difference) modes are higher-order modes with frequency ω equal to $\omega_i \pm \omega_j$, the sum (difference) of fundamental frequencies ω_i. Their intensities are temperature dependent according to $(n_i+\frac{1}{2}) \pm (n_j+\frac{1}{2})$, where n_i is the Bose factor, $n_i+\frac{1}{2}=\frac{1}{2}\coth(\hbar\omega_i/2k_BT)$, with a temperature T and the Boltzmann constant k_B. The following features can be observed in the spectra: (i) besides four first-order peaks there are more than 180 weak absorptions; (ii) no difference peaks are resolved (i.e., no temperature

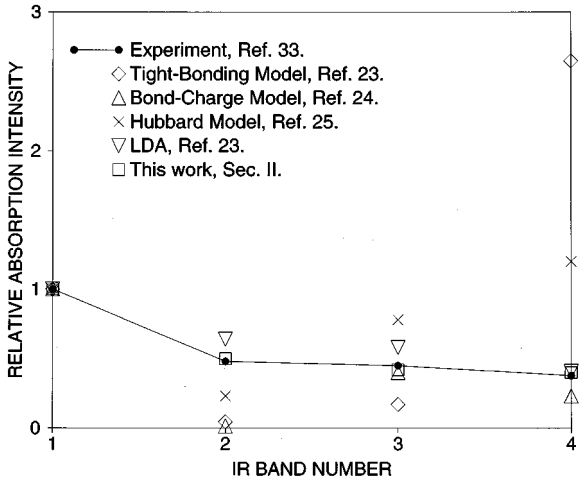

FIG. 1. Comparison of calculated relative absorption intensities of IR-allowed $T_{1u}(i)$, $i=1$, 2, 3, and 4, modes with experiment. Intensities of the band $T_{1u}(1)$ are taken to be unity.

dependence of intensities except a trivial improvement in the frequency resolution at lower temperatures); (iii) most of the spectral weight is in the high-frequency regime (1000–3000 cm^{-1}); and (iv) weak modes around four first-order bands are not enhanced through a resonance effect.

This paper treats the frequency positions and absorption intensities independently. Normal modes and frequencies are calculated using a simple force-constant model proposed by Weeks.[27] This model fits IR data reasonably well but is not expected to give especially realistic eigenfrequencies for the silent modes. The dipole moment that arises due to the electron-phonon coupling determines the absorption intensities.[28] Only second-order combination and difference modes are considered in the paper. Section II deals with the mechanical anharmonicity problem with the Morse function used for the interatomic bond-stretching potential.[27] A linear relation between the dipole moment and ionic coordinates is proposed in this section. The relation contains parameters fittable to the relative harmonic absorption intensities. Second-order modes are computed using a perturbation method ignoring possible resonances. However, the intensity pattern of the second-order modes fails to reproduce experimental features. An electrical anharmonicity model is therefore introduced in Sec. III. Normal frequencies and normal modes are again taken to be those of the Weeks model. A semiempirical model for an electronic configuration on a distorted C_{60} is presented, which allows the electronic coordinates to depend in a nonlinear fashion on positions of ions. This gives rise to an intensity pattern very similar to the experimental one. Finally, conclusions are drawn in Sec. IV.

II. MECHANICAL ANHARMONICITY MODEL

Considering the C_{60} molecule as a system of oscillating ions with electrons moving adiabatically in their field, the ionic dynamics is governed by the following potential:

$$V=\frac{1}{2}\sum_{i=1}^{46}\sum_{q=1}^{g_i} m\omega_i^2 Q_{iq}^2 + \frac{1}{6}\sum_{i,j,k=1}^{46}\sum_{q,r,s=1}^{g_i,g_j,g_k} C_{iq,jr,ks}Q_{iq}Q_{jr}Q_{ks}. \quad (1)$$

Here m is the ion mass, Q_{iq} is the qth normal mode coordinate belonging to the frequency ω_i, $i=1,\ldots,46$, $q=1,\ldots,g_i$, and g_i is the degeneracy of the ith band. Higher-order terms are neglected. The anharmonicity coefficients $C_{iq,jr,ks}$ are given by

$$C_{iq,jr,ks}=\frac{\partial^3 V}{\partial Q_{iq}\partial Q_{jr}\partial Q_{ks}}. \quad (2)$$

Light couples to the system via the term

$$V_1=-\mu(Q)\cdot\mathbf{E}, \quad (3)$$

where $\mathbf{E}$ is the externally applied macroscopic electric field and μ stands for the dipole moment of the system. The latter is generally a nonlinear function of normal coordinates

$$\mu=\sum_{i=1}^{46}\sum_{q=1}^{g_i}\mathbf{M}_{iq}Q_{iq}+\frac{1}{2}\sum_{j,k=1}^{46}\sum_{r,s=1}^{g_j,g_k}\mathbf{M}_{jr,ks}Q_{jr}Q_{ks}. \quad (4)$$

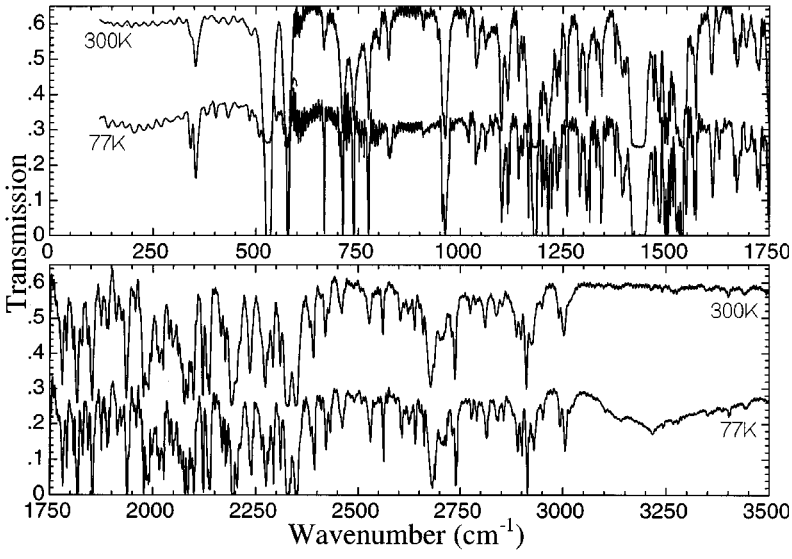

FIG. 2. C_{60} single-crystal IR transmission spectra at 300 and 77 K by Martin *et al.* (Ref. 8).

Again, higher-order terms are not included and the following formulas determine the expansion parameters $\mathbf{M}_{iq}$ and $\mathbf{M}_{jr,ks}$:

$$\mathbf{M}_{iq}=\frac{\partial\mu}{\partial Q_{iq}}, \tag{5}$$

and

$$\mathbf{M}_{jr,ks}=\frac{\partial^2\mu}{\partial Q_{jr}\partial Q_{ks}}. \tag{6}$$

The vectors $\mathbf{M}_{iq}$ are nonzero only when the Q_{iq} mode is IR allowed.

Anharmonic dynamics ($C_{iq,jr,ks}\neq 0$) and a linear coupling of light to phonons ($\mathbf{M}_{kr,ls}=0$) characterize the mechanical anharmonicity (MA) phenomenon.

Several force-constant models for C_{60} have been presented.[27,29,30] To calculate normal coordinates and the anharmonicity coefficients $C_{iq,jr,ks}$, I use the model suggested by Weeks,[27] which is a refined model of Weeks and Harter.[31] This model contains two parameters that were fitted to selected IR and Raman frequencies. Ionic dynamics is governed by two types of interactions: (i) The Morse potential producing anharmonic terms

$$V_m=\sum_{i=1}^{90} D\{1-\exp[-\alpha(r_i-r_{\rm eq})]\}^2, \tag{7}$$

controls bond stretching. Here D, α, $r_{\rm eq}$, and r_i are, respectively, the dissociation energy, Morse anharmonicity, equilibrium, and instantaneous length of the ith bond. Summation runs over all bonds. The dissociation energy is estimated as the average of the dissociation energies of a single and a double C_2 bond, $D=5.0$ eV, the equilibrium length is taken to be 1.4 Å, and the parameter α was fitted to the value 1.6 Å^{-1}. (ii) The bond-bending harmonic potential is given by

$$V_b=\sum_j \eta(\theta_{\rm eq}-\theta_j)^2, \tag{8}$$

where the summation is over the 60 pentagonal angles with the equilibrium angle of $\frac{3}{5}\pi$ and the 120 hexagonal angles with the equilibrium angle of $\frac{2}{3}\pi$. The potential does not distinguish between hexagonal and pentagonal angles and the best fit yields $\eta=12.48$ eV/rad.

The bond-stretching potential in the harmonic approximation together with the bond-bending potential give normal coordinates and frequencies. The coefficients $C_{iq,jr,ks}$ come from the expansion of the Morse function to the third order in ionic distortions from equilibrium and from the transformation of the Cartesian coordinates to the normal mode ones computed numerically. Qualitative behavior of the normal modes of the model (with the bond-stretching potential in the harmonic approximation) is discussed in the original papers.[27,31] It is enough to note that lower-frequency normal modes exhibit mostly radial distortions while the motion of higher-frequency ones is tangential.

The IR intensity of a given mode is proportional to the square of a dipole moment associated with the mode. If ionic charges of the same value were put on the vertices of C_{60}, the resulting dipole moment would be zero due to the center-of-mass conservation. The dipole activity is therefore caused by changes in the electronic configuration. Carbon valence electrons fall into two classes. The first class consists of σ electrons positioned with the highest probability in the middle of bonds. These electrons have fixed charges and do not contribute to the dipole moment (due to the center-of-mass conservation). In the following the notion of a bond charge will include also a contribution from ions in some effective way. The sign of such an effective bond charge will not be important; it can be either positive or negative. Allowing the bond charges to acquire a charge with dependence on the bond lengths or by some other mechanism leads to a spectrum where the $T_{1u}(2)$ mode is hardly visible instead of having the second largest activity.[24,32] The second class consists of π electrons that create a dipole moment in the following way. Consider these π electrons to be vertex electrons moving in the field of their parent ions. Let these electrons interact further only with the three nearest ions. The positions of the π electrons are modeled in the following way. Let $\mathbf{r}_i$ denote the radius vector of the ith electron measured from the vertex i with the position $\mathbf{R}_i$ and $\mathbf{R}_j^{(i)}$, $j=1,2,3$, the nearest ions positions, respectively, seen from the center of C_{60}. The direction of $\mathbf{r}_i$ is taken to be the direction of the normal vector $\mathbf{n}_i$ to the plane given by three nearest ions with a rescaled position of the one making the double bond with the vertex. This condition,

$$\mathbf{n}_i\cdot(\mathbf{R}_1^{(i)}-\mathbf{R}_2^{(i)})=\mathbf{n}_i\cdot(\mathbf{R}_1^{(i)}-c_1\mathbf{R}_3^{(i)})=0, \tag{9}$$

introduces a fitting parameter c_1, effectively measuring the ratio of the double- and single-bond charge (here the bond $\mathbf{R}_i-\mathbf{R}_3^{(i)}$ is the double one). Single bonds are bonds connecting a hexagon with a pentagon and double bonds are connecting two hexagons. When there is more charge on the double bond than on the single one, the parameter c_1 is greater than unity. If the bond charge is negative, the direction is out of the sphere and if it is positive, the direction is inwards.

Consider the distance d of the vertex ion to the plane given by its three nearest ionic neighbors (with the double-bond neighbor rescaled as explained above). Denote as $d_{\rm eq}$ the distance for the equilibrium configuration. Let, for a moment, the effective bond charge be negative. If a distortion of the ionic positions occurs such that $d>d_{\rm eq}$ the vertex electron will be pushed ''out'' of the C_{60} sphere and vice versa. If the net bond charge is positive, the situation is inverse. This phenomenology reflects a Coulomb repulsion (attraction) of the vertex electron by (to) adjacent bonds. When these bonds move closer together the vertex electronic cloud is deformed such that the mean electronic position will be as far (close) as possible from (to) the bonds. The effective rate of the deformation will be the second free parameter c_2 (the same for each vertex due to symmetry). The relation between the electronic position and the distance between the vertex ion and the plane given by its nearest neighbors can then be expressed as follows:

$$\mathbf{r}_i=\{1+c_2[d_i(c_1)-d_{\rm eq}(c_1)]\}\mathbf{n}_i(c_1), \tag{10}$$

where the dependence on the parameter c_1 is indicated. The dipole moment is then clearly

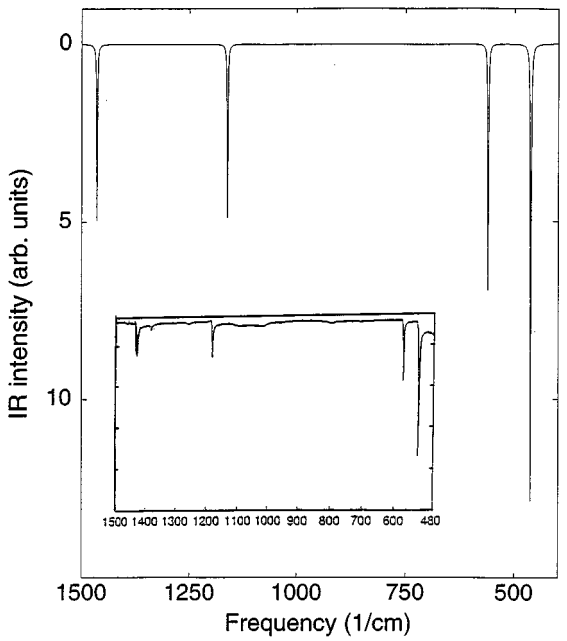

FIG. 3. First-order IR-allowed intensities calculated in Sec. II and experimentally obtained spectrum (inset) by Hare *et al.* (Ref. 6).

$$\mu=\sum_{i=1}^{60}\left[1+c_2(d_i-d_{\mathrm{eq}})\right]\mathbf{n}_i\,. \tag{11}$$

The normalization in both formulas is not important for calculating relative values. The distances d_i depend for small distortions linearly on normal coordinates, so only the linear term is kept here because the mechanical anharmonicity couples this linear displacement to two normal modes.

There are two natural parameters in this model, c_1 and c_2. In the harmonic approximation the intensity of the jth mode is[28]

$$I^{(1)}_{\omega_j}=\sum_{q=1}^{g_j}\mathbf{M}^2_{jq}\,. \tag{12}$$

Experimentally obtained relative intensities are 1, 0.48, 0.45, and 0.378 for the modes $T_{1u}(1)$, $T_{1u}(2)$, $T_{1u}(3)$, and $T_{1u}(4)$, respectively.[33] The best fit to these intensities yields the values $c_1=1.59$ and $c_2=0.67$ Å^{-1}. The IR spectrum obtained with the fit (all peaks in this and the following figures have the Lorentzian widths taken to be uniformly 2 cm^{-1}) along with an experimental one is shown in Fig. 3. Agreement with experiment is very good.

For the frequencies that are not in the immediate neighborhood of the frequencies of the four IR-allowed fundamentals, the following formulas were obtained in Ref. 18 for the second-order intensities of combination and difference modes:

$$I^{\mathrm{MA}}_{\omega_k+\omega_l}=\frac{\hbar}{2m^3}\frac{\omega_k+\omega_l}{\omega_k\omega_l}(1+n_k+n_l)\times\sum_{r,s=1}^{g_k,g_l}\left(\sum_{j\in\mathrm{IR}}\frac{\langle\mathbf{M}_j|C_{j,kr,ls}\rangle}{\omega_j^2-(\omega_k+\omega_l)^2}\right)^2, \tag{13}$$

and

$$I^{\mathrm{MA}}_{\omega_l-\omega_k}=\frac{\hbar}{2m^3}\frac{\omega_l-\omega_k}{\omega_k\omega_l}(n_k-n_l)\times\sum_{r,s=1}^{g_k,g_l}\left(\sum_{j\in\mathrm{IR}}\frac{\langle\mathbf{M}_j|C_{j,kr,ls}\rangle}{\omega_j^2-(\omega_l-\omega_k)^2}\right)^2, \tag{14}$$

respectively. The summation in brackets is over four IR-active bands and the inner-product notation stands for the sum over a degenerate set:

$$\langle\mathbf{M}_j|C_{j,\ldots}\rangle\equiv\sum_{q=1}^{g_j}\mathbf{M}_{jq}C_{jq,\ldots}\,. \tag{15}$$

When the frequency of a combination (difference) mode is near the frequency of an IR-allowed mode (the Fermi resonance effect), a perturbation leads to a mixing of the two modes and spreads out their frequencies (see Ref. 16). The second-order modes are enhanced, conserving the original spectral weight so the integrated absorption intensity of the band is unchanged by the anharmonic perturbation. If the spectral resolution is not enough to resolve the two modes the resulting picture is similar to the original one without a perturbation. The Fermi resonance effect has not been observed in C_{60}.

Figure 4 shows the results of the numerical calculations based on the Eqs. (12)–(14). Some trends in the spectrum are clear already from the equations. First of all the second-order intensities are relatively weak compared to the experimental spectrum in Fig. 2 (the experimental picture here is somewhat misleading due to the saturation of first-order peaks). Most intense modes have frequencies close to the four IR bands, leaving high-frequency combination modes practically invisible. Moreover there are relatively intense difference modes (identified by their strong temperature dependence) in the lower part of the spectrum. These features are in contradiction to experiment, thus excluding mechanical anharmonicity as the mechanism for activation of the combination modes seen in experiment. In matching the combination modes to experimental data, the authors in Ref. 8 did not find any evidence for a significant deviation of the frequencies of these modes from the values of $\omega_i+\omega_j$. This supports the above conclusion that mechanical anharmonicity is not producing significant effects in the C_{60} IR spectrum, since the relative frequency shift as a consequence of mechanical anharmonicity only is of the same order of magnitude as the relative intensities of the second-order modes.

III. ELECTRICAL ANHARMONICITY MODEL

The electrical anharmonicity (EA) is a less studied phenomenon of molecular physics than the mechanical one. It is based on the fact that the dipole moment is generally a nonlinear function of normal modes. In view of Eqs. (1) and (4), electrical anharmonicity arises from the second term in Eq. (4), while the ionic dynamics is harmonic ($C_{iq,jr,ks}=0$). Selection rules for the second-order modes are reflected in the elements of the matrix $\mathbf{M}_{jr,ks}$, and are the same as in the case of the mechanical anharmonicity. Since the ionic dipole moment is linear in ionic positions it is clear that the nonlinear contribution stems from a nonlinear response of electronic positions to a change in ionic configuration. A har-

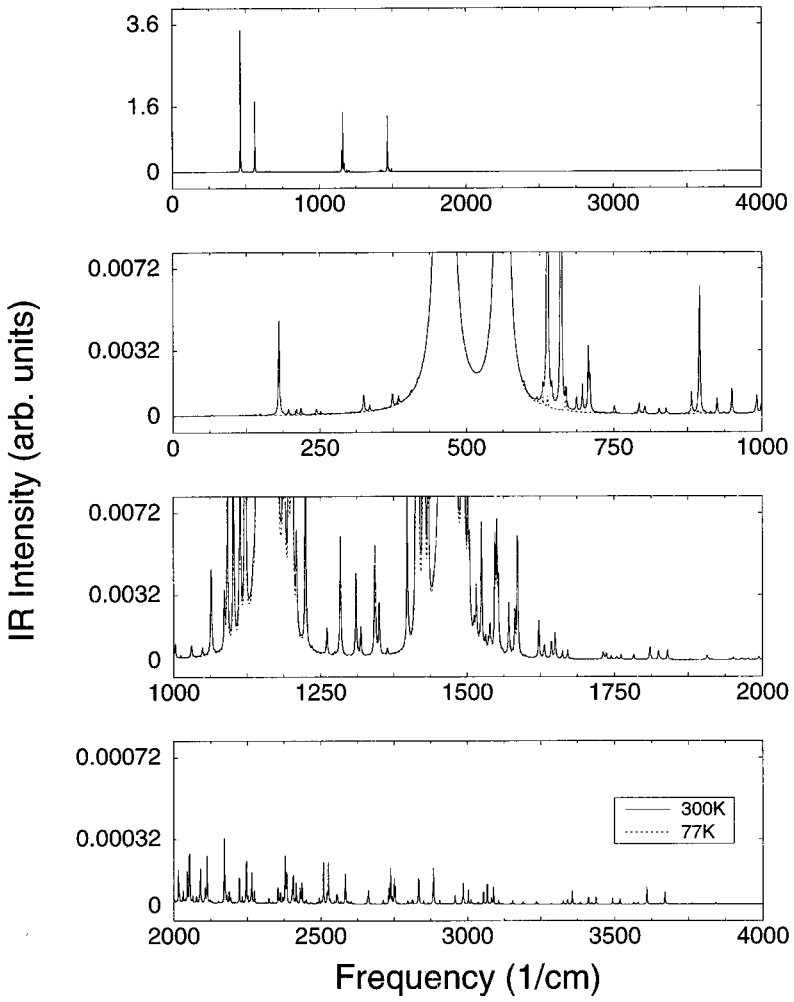

FIG. 4. IR spectra at 300 and 77 K computed using the mechanical anharmonicity model introduced in Sec. II. Difference modes are easily identified by their strong temperature dependence, while combination modes show no such trends.

monic treatment now suffices for the ionic displacements; the Weeks model of Sec. II is used.

The nonlinear electronic response is modeled in the following way. The notation is the same as in the previous section. Consider again a π electron in the field of its parent ion and adjacent bond charges. The interaction with its nearest-neighbor ions is governed by the Coulomb potential

$$V_{e\text{-}i}(\mathbf{r}_i) = -\kappa_i \sum_j \frac{1}{|\mathbf{R}_i - \mathbf{R}_j + \mathbf{r}_i|} \tag{16}$$

and similarly the interaction with adjacent bond electrons is given by

$$V_{e\text{-}be}(\mathbf{r}_i) = \kappa_{be} \sum_j \frac{1}{|(\mathbf{R}_i - \mathbf{R}_j)/2 + \mathbf{r}_i|}. \tag{17}$$

The summations are over the three nearest ions and $\mathbf{R}_i$ is the position of the vertex ion. Note that while $\mathbf{R}$'s are measured from the mass center of C_{60}, $\mathbf{r}_i$ is measured from the position of the ith vertex ion ($\mathbf{R}_i$). The strengths of the interactions are measured by some effective charges κ_i and κ_{be} for neighbor ions and adjacent bond electrons, respectively. Only the ratio κ_i/κ_{be} is a relevant fitting parameter. The motion of the π electron in the field of its vertex ion is simplified by restricting it to a sphere around the ion with a radius R, which will be the second fitting parameter:

$$\mathbf{r}_i = R\mathbf{n}_i . \tag{18}$$

This gives a simple two-dimensional minimization scheme: for each vertex and a pair of fitting parameters $(R, \kappa_i/\kappa_{be})$ find a unit vector $\mathbf{n}_i$ such that the function

$$V_{e\text{-}i}(\mathbf{n}_i) + V_{e\text{-}be}(\mathbf{n}_i) \tag{19}$$

is minimal. The electrical dipole moment is then computed and resulting first-order intensities [Eq. (12)] are compared with corresponding experimental values. The best fit corresponds to values of $R = 0.06$ Å and $\kappa_i/\kappa_{be} = 4.80$. For some range of the parameters there are two electron positions for which the potential in Eq. (19) has a local minimum. In such cases the global one was considered. The best fit lies in the region with one minimum. It is obvious that the best fits have no physical justification. To support the model I did simulations with different, more physical values of the free parameters obtaining the same qualitative picture as will be shown later. It is also appropriate to remark that a feedback from the adiabatic changes in electronic positions to ionic motion is implicitly considered in the harmonic level in the force-constant model.

For the IR absorption the changes of the minima positions with ionic distortions are relevant. Numerical differentiation was used to obtain the dipole-moment matrices $\mathbf{M}_{iq}$ and $\mathbf{M}_{jr,ks}$ from Eqs. (5) and (6). An important feature of the

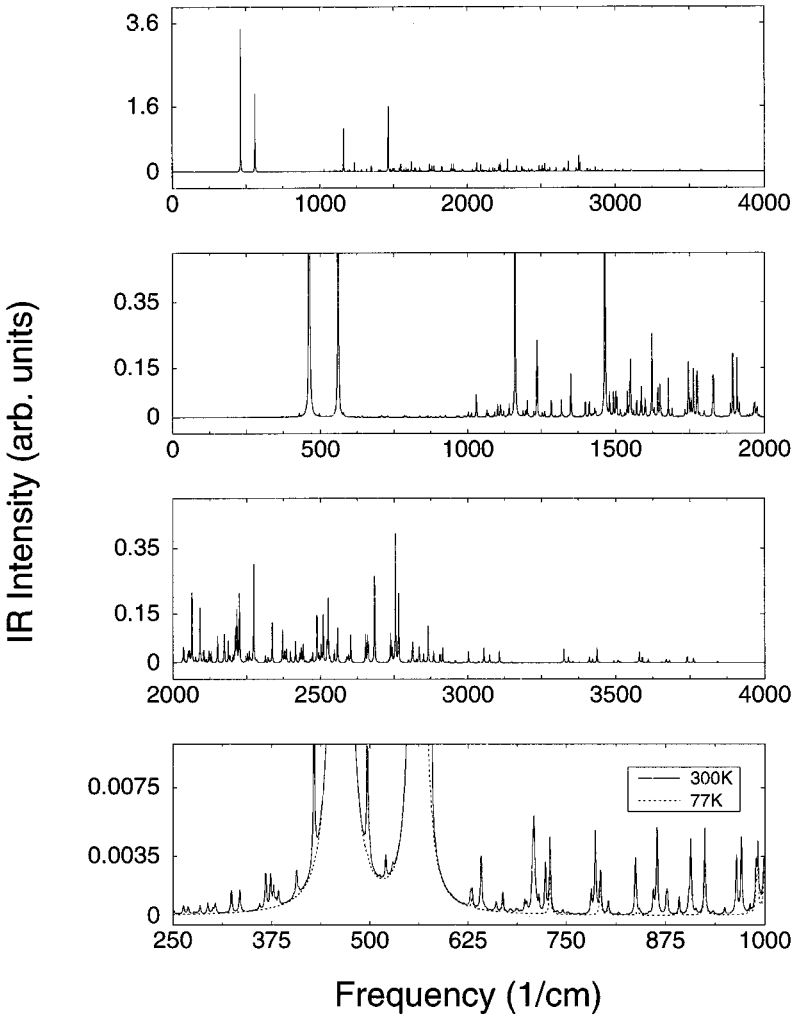

FIG. 5. The electronic anharmonicity model (Sec. III) produces absorption spectra that show similar trends as experimental ones. Difference peaks carry very little spectral weight compared to high-frequency combination ones.

model is that the π-electronic positions are more sensitive to tangential distortions than to radial ones.

Second-order absorption intensities of combination and difference modes now have simple forms:[18]

$$I^{\mathrm{EA}}_{\omega_k+\omega_l}=\frac{\hbar}{2m}\,\frac{\omega_k+\omega_l}{\omega_k\omega_l}(1+n_k+n_l)\sum_{r,s=1}^{g_k,g_l}\mathbf{M}^2_{kr,ls}\,, \qquad (20)$$

$$I^{\mathrm{EA}}_{\omega_k-\omega_l}=\frac{\hbar}{2m}\,\frac{\omega_k-\omega_l}{\omega_k\omega_l}(n_l-n_k)\sum_{r,s=1}^{g_k,g_l}\mathbf{M}^2_{kr,ls}\,. \qquad (21)$$

Figure 5 shows the spectrum obtained from Eqs. (20) and (21). The following features can be extracted. The overall intensity of the weak modes is higher (in a relative sense) than in the case of the mechanical anharmonicity. Spectral weight is shifted towards higher frequencies. This is a consequence of high sensitivity of electronic positions to tangential distortions, which are characteristic for higher-frequency modes. The sensitivity of electrons to the tangential ionic motion is also the reason that difference peaks have relatively very small intensity (the difference peaks are most intense in the region of 600–1000 cm^{-1}, however, the intensities are much smaller than those of combination modes in the region 1000–3500 cm^{-1}). There is obviously no resonance effect since the two terms in Eq. (4) are independent. The frequency distribution in the Weeks model differs from that in C_{60} so a closer comparison with experiment is not possible. One consequence is that in Fig. 5 weak features up to 4000 cm^{-1} are visible, while experimentally weak peaks above 3500 cm^{-1} have not been resolved. This difference in the frequency distribution may be a part of the reason that there is so little activity in the region 600–1000 cm^{-1}. Note that almost all of the peaks experimentally observed in this region were associated with modes IR forbidden in the second order[7,8] and their appearance must be accounted for by other mechanisms.

IV. CONCLUSION

Mechanical and electrical anharmonicity provide possible mechanisms for activating weak modes resolved in IR spectra of C_{60} thin films and single crystals. I have proposed simple semiempirical models of the phenomena. The main features of the models are (i) separation of ionic dynamics and mechanism of optical activation (the models can be used for any set of normal modes), and (ii) emphasis on the π-electronic system rather than on bond charges. Both models give a spectrum of combination and difference modes that is compared with IR measurements. It is found that mechanical anharmonicity exhibits features different from those observed. These features can be generally expected from basic formulas [e.g., those of Eqs. (13) and (14)] and the model

described in Sec. II only helps to visualize them. As a by-product the intensities of four first-order IR-allowed bands are well reproduced.

The electrical anharmonicity model introduced in Sec. III is based on a nonlinear response of π-electronic configuration to ionic distortions. Now the absorption spectrum has fewer characteristics given *a priori* by a theoretical formula and is more model dependent. The main feature of the model, which leads to a quite successful comparison of its spectrum with experiment, is that electronic positions are much more sensitive to tangential ionic motions than to radial ones.

The separation of mechanical and electrical anharmonicity is posteriorly justified by the dominance of the latter. However, the IR activity around four first-order peaks is caused by mechanical anharmonicity due to resonance effects, as discussed in Sec. II. There is still a region of optical activity (600–1000 cm^{-1}) that this simple model cannot explain. Although trial assignments exclude most of the observed peaks in the region as combination modes, the question is still an open one and more sophisticated quantum-mechanical treatment can yield more authoritative results.

ACKNOWLEDGMENTS

I am grateful to P. B. Allen for proposing this study. I thank M. C. Martin and L. Mihaly for useful discussions. This work was supported by NSF Grant No. DMR 9417755.

[1] A. F. Hebard, M. J. Rosseinsky, R. C. Haddon, D. W. Murphy, S. H. Glarum, T. T. M. Palstra, A. P. Ramirez, and A. R. Kortan, Nature **350**, 600 (1991).

[2] M. Schlüter, M. Lannoo, M. Needels, G. A. Baraff, and D. Tománek, J. Phys. Chem. Solids **53**, 1473 (1992); M. Schlüter, M. Lannoo, M. Needels, and G. A. Baraff, Phys. Rev. Lett. **68**, 526 (1992); C. M. Varma, J. Zaanen, and K. Raghavachari, Science **254**, 989 (1991).

[3] S. Chakravarty, M. Gelfand, and S. Kivelson, Science **254**, 970 (1991); S. Chakravarty and S. Kivelson, Europhys. Lett. **16**, 751 (1991).

[4] W. Kratschmer, K. Fostiropoulos, and D. R. Huffman, Chem. Phys. Lett. **170**, 167 (1990).

[5] D. S. Bethune, G. Meijer, W. C. Tang, H. J. Rosen, W. G. Golden, H. Seki, C. A. Brown, and M. S. de Vries, Chem. Phys. Lett. **179**, 181 (1991).

[6] J. P. Hare, J. Denis, H. W. Kroto, R. Taylor, A. W. Allaf, S. Balm, and D. R. M. Walton, J. Chem. Soc. Chem. Comm. **1**, 412 (1991).

[7] K.-A. Wang, A. M. Rao, P. C. Eklund, M. S. Dresselhaus, and G. Dresselhaus, Phys. Rev. B **48**, 11 375 (1993).

[8] M. C. Martin, X. Q. Du, J. Kwon, and L. Mihaly, Phys. Rev. B **50**, 173 (1994).

[9] K. Kamarás, L. Akselrod, S. Roth, A. Mittelbach, W. Hönle, and H. G. von Schnering, Chem. Phys. Lett. **214**, 338 (1993).

[10] Z.-H. Dong, P. Zhou, J. M. Holden, P. C. Eklund, M. S. Dresselhaus, and G. Dresselhaus, Phys. Rev. B **48**, 2862 (1993).

[11] P. H. M. van Loosdrecht, P. J. M. van Bentum, M. A. Verheijen, and G. Meijer, Chem. Phys. Lett. **198**, 587 (1992); P. H. M. van Loosdrecht, P. J. M. van Bentum, M. A. Verheijen, and G. Meijer, Phys. Rev. Lett. **68**, 1176 (1992).

[12] B. Chase, N. Herron, and E. Holler, J. Phys. Chem. **96**, 4262 (1992).

[13] C. Coulombeau, H. Jobic, P. Bernier, C. Fabre, D. Schütz, and A. Rassat, J. Phys. Chem. **96**, 22 (1992); J. R. D. Copley, D. A. Neumann, R. L. Cappelletti, and W. A. Kamitakahara, J. Phys. Chem. Solids **53**, 1353 (1992).

[14] M. C. Martin, J. Fabian, J. Godard, P. Bernier, J. M. Lambert, and L. Mihaly, Phys. Rev. B **51**, 2844 (1995).

[15] L. Mihaly and M. C. Martin, in *Proceedings of the 1955 International Winterschool on Electronic Properties of Novel Materials: Fullerides and Fulleroids*, edited by H. Kuzmany, J. Fink, M. Mehring, and S. Roth (World Scientific, Singapore, 1995).

[16] G. Herzberg, *Infrared and Raman Spectra of Polyatomic Molecules* (van Nostrand, New York, 1966).

[17] M. Lax and E. Burstein, Phys. Rev. **97**, 217 (1955).

[18] B. Szigeti, Proc. R. Soc. London Ser. A **252**, 217 (1959); **258**, 377 (1960).

[19] B. Szigeti, in *Lattice Dynamics*, edited by R. F. Wallis (Pergamon, New York, 1963), p. 405.

[20] D. L. Mills, C. J. Duthler, and M. Sparks, in *Dynamical Properties of Solids*, edited by G. K. Horton and A. A. Maradudin (North-Holland, Amsterdam, 1980), Vol. 4, p. 377, and references therein.

[21] M. Sparks, Phys. Rev. B **10**, 2581 (1974).

[22] B. Friedman, Mol. Cryst. Liq. Cryst. **256**, 251 (1994).

[23] G. F. Bertsch, A. Smith, and K. Yabana, Phys. Rev. B **52**, 7876 (1995).

[24] S. Sanguinetti, G. Benedek, M. Righetti, and G. Onida, Phys. Rev. B **50**, 6743 (1994).

[25] M. I. Salkola, S. Chakravarty, and S. Kivelson, Int. J. Mod. Phys. **7**, 2859 (1993).

[26] P. Giannozi and S. Baroni, J. Chem. Phys. **100**, 8537 (1994).

[27] D. Weeks, J. Chem. Phys. **96**, 7380 (1992).

[28] E. B. Wilson, J. C. Decius, and P. C. Cross, *Molecular Vibrations* (Dover, New York, 1980), p. 162.

[29] Z. C. Wu, D. A. Jelski, and T. F. George, Chem. Phys. Lett. **137**, 291 (1987); S. J. Cyvin, E. Brendsdal, B. N. Cyvin, and J. Brunvoll, *ibid.* **43**, 377 (1988).

[30] G. Onida and G. Benedek, Europhys. Lett. **18**, 403 (1992); **99**, 343 (1992); R. A. Jishi, R. M. Mirie, and M. S. Dresselhaus, Phys. Rev. B **45**, 13 685 (1992); J. L. Feldman, J. Q. Broughton, L. L. Boyer, D. E. Reich, and M. D. Kluge, *ibid.* **46**, 12 731 (1992); D. W. Snoke and M. Cardona, Solid State Commun. **87**, 121 (1993); D. Inomata, N. Kurita, S. Suzuki, and K. Nakao, Phys. Rev. B **51**, 4533 (1995).

[31] D. E. Weeks and W. G. Harter, Chem. Phys. Lett. **144**, 366 (1988); **176**, 209 (1991).

[32] J. Fabian (unpublished).

[33] M. C. Martin, D. Koller, and L. Mihaly, Phys. Rev. B **47**, 14 607 (1993).